

# The kinematics and the origin of the ionized gas in NGC 4036

By E. M. CORSINI<sup>1</sup>, F. BERTOLA<sup>1</sup>, M. SARZI<sup>1</sup>,  
 P. CINZANO<sup>1</sup>, H.-W. RIX<sup>2</sup> AND W.W. ZEILINGER<sup>3</sup>

<sup>1</sup>Dipartimento di Astronomia, Università di Padova, Vicolo dell'Osservatorio 5, I-35122 Padova, Italy

<sup>2</sup>Steward Observatory, University of Arizona, Tucson, AZ-85721

<sup>3</sup>Institut für Astronomie, Universität Wien, Türkenschanzstrasse 17, A-1180 Wien, Austria

The kinematics of stars and ionized gas has been studied near the center of the S0 galaxy NGC 4036. Dynamical models based both on stellar photometry and kinematics have been built in order to derive the gravitational potential in which the gas is expected to orbit. The observed gas rotation curve falls short of the circular velocity curve inferred from these models. Inside 10'' the observed gas velocity dispersion is found to be comparable to the predicted circular velocity, showing that the gas cannot be considered on circular orbits. The understanding of the observed gas kinematics is improved by models based on the Jeans Equations, which assume the ionized gas as an ensemble of collisionless clouplets distributed in a spheroidal and in a disk component.

## 1. Introduction

NGC 4036 has been classified S0<sub>3</sub>(8)/Sa in RSA (Sandage & Tammann 1981) and S0<sup>-</sup> in RC3 (de Vaucouleurs *et al.* 1991). Its total apparent magnitude is  $V_T = 10.66$  mag (RC3). This corresponds to a total luminosity  $L_V = 4.2 \cdot 10^{10}$   $L_\odot$  at the assumed distance of  $d = V_0/H_0 = 30.2$  Mpc, where  $V_0 = 1509 \pm 50$  km s<sup>-1</sup> (RSA) and assuming  $H_0 = 50$  km s<sup>-1</sup> Mpc<sup>-1</sup>. At this distance the scale is 146 pc arcsec<sup>-1</sup>.

We measured the kinematics of stars and ionized gas along the galaxy major axis and we also derived their distribution in the nuclear regions by means of ground-based *V*-band and HST narrow-band imaging respectively.

## 2. Modeling the stellar kinematics

We apply to the observed stellar kinematics the Jeans modeling technique introduced by Binney *et al.* (1990), developed by van der Marel *et al.* (1990) and van der Marel (1991), and extended to two-component galaxies by Cinzano & van der Marel (1994).

The best-fit model to the observed major-axis stellar kinematics is shown in Fig. 1. The bulge is an oblate isotropic rotator ( $k = 1$ ) with  $(M/L_V)_b = 3.4$  (M/L)<sub>○</sub>. The exponential disk has  $(M/L_V)_d = 3.4$  (M/L)<sub>○</sub> with the velocity dispersion profile given by  $\sigma_*(r) = 155 e^{-r/r_\sigma}$  km s<sup>-1</sup> with scale-length  $r_\sigma = 27.4'' = 4.0$  kpc. The derived bulge and disk masses are  $M_b = 9.8 \cdot 10^{10}$   $M_\odot$  and  $M_d = 4.8 \cdot 10^{10}$   $M_\odot$ , adding up to a total (bulge+disk) luminous mass of  $M_T = 14.5 \cdot 10^{10}$   $M_\odot$ . The disk-to-bulge and disk-to-total luminosity ratios are  $L_b/L_d = 0.58$  and  $L_d/L_T = 0.36$ .

## 3. Modeling the gaseous kinematics

At small radii both the ionized gas velocity and velocity dispersion are comparable to stellar velocity and velocity dispersion, for  $r \leq 9''$  and  $r \leq 5''$  respectively. Moreover a

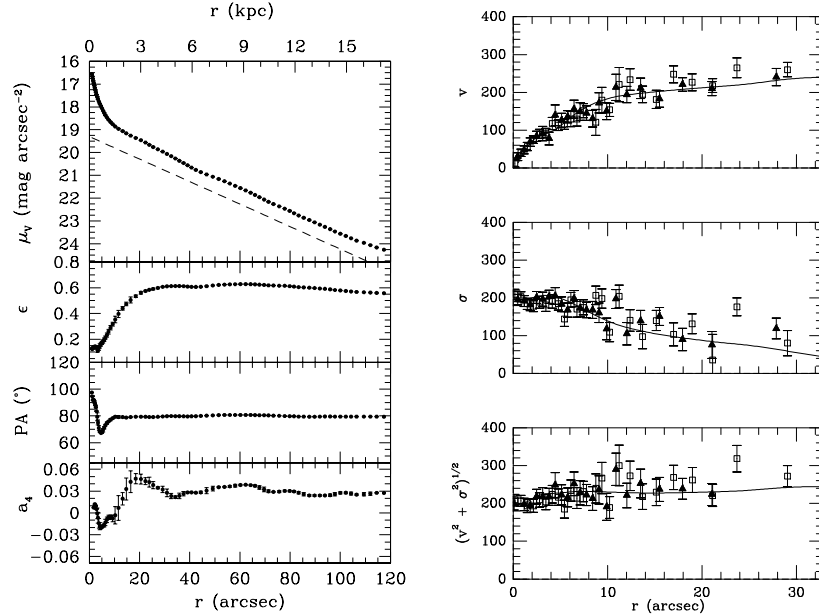


FIGURE 1. *Left panel:* Ground-based  $V$ -band surface-brightness, ellipticity, position angle and  $\cos 4\theta$  coefficient radial profiles of NGC 4036. The dashed line represents the surface-brightness profile of the exponential disk adopted in our dynamical model. *Right panel:* Comparison of the model predictions to the stellar major-axis kinematics for NGC 4036

change in the slope of the [O II]  $\lambda 3726$  intensity radial profile is observed inside  $r \simeq 8''$ , its gradient appears to be somewhat steeper towards the center. The velocity dispersion and intensity profiles of the ionized gas suggest that it is distributed into two components: a small inner spheroidal component and a disk. We decomposed the [O II]  $\lambda 3726$  intensity profile as the sum of an  $R^{1/4}$  gaseous spheroid and an exponential gaseous disk and the gas spheroid resulted to be the dominating component up to  $r \simeq 8''$ .

We built up dynamical models for the ionized gas in NGC 4036 (Fig. 2). It was assumed to be distributed in a dynamically hot spheroidal and in a dynamically cold disk component and consisting of collisionless individual clumps (cloudlets) which orbit in the total potential. We made two different sets of assumptions based on two different physical scenarios for the gas cloudlets.

*Model A:* In a first set of models we described the gaseous component consisting of collisionless cloudlets which can be considered in hydrostatic equilibrium. The gaseous spheroid is characterized by a density distribution and flattening different from those of stars. Its major-axis luminosity profile was assumed to follow an  $R^{1/4}$  law. The flattening of the spheroid  $q$  was kept as free parameter. To derive the kinematics of the gaseous spheroid and disk we solved the Jeans Equations.

*Model B:* In a second set of model we assumed that the emission observed in the gaseous spheroid and disk arise from material that was recently shed from stars. Different authors (Bertola *et al.* 1984, 1995b; Fillmore *et al.* 1986; Kormendy & Westpfahl 1989; Mathews 1990) suggested that the gas lost (e.g. in planetary nebulae) by stars was heated by shocks to the virial temperature of the galaxy within  $10^4$  years, a time shorter than the typical dynamical time of the galaxy. Hence in this picture the ionized gas and the stars have the same true kinematics, while their observed kinematics are different due to the line-of-sight integration of their different spatial distribution.

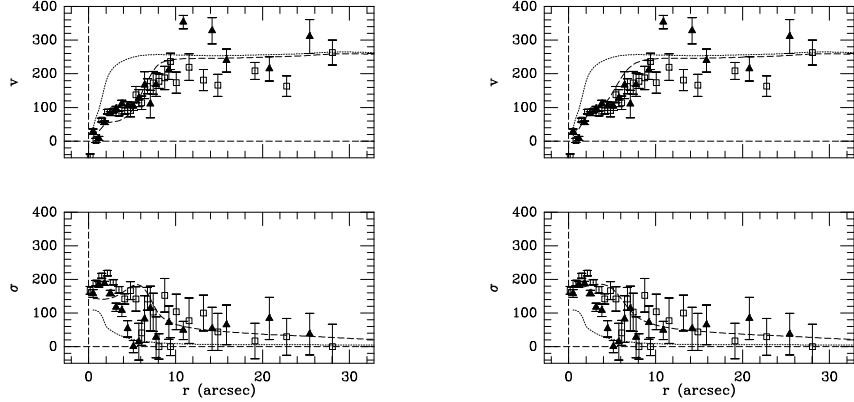


FIGURE 2. Comparison of the predictions (dashed curves) of model A (left panel) and model B (right panel) to the ionized gas kinematics observed along the major axis of NGC 4036. The dotted curves represent the seeing-convolved circular velocity curve and zero velocity-dispersion profile in the galaxy meridional plane respectively

#### 4. Do drag forces affect the kinematics of the gaseous cloudlets?

The discrepancy between model and observations could be explained by taking properly into account the drag interaction between the ionized gas cloudlets of the gaseous spheroid and the hot component of the interstellar medium (Mathews 1990). To have some qualitative insights in understanding the effects of a drag force on the gas kinematics we studied the case of a gaseous nebula moving in the spherical potential generated by an homogeneous mass distribution of density  $\rho$  and which, starting onto a circular orbit, is decelerated by a drag force  $\mathbf{F}_{drag} = -(k_{drag}v/m)\mathbf{v}$ , where  $m$  and  $\mathbf{v}$  are the mass and the velocity of the gaseous cloud and the constant  $k_{drag}$  is given following Mathews (1990). We numerically solved the equations of motion of a nebula to study the time-dependence of the radial and tangential velocity components  $\dot{r}$  and  $r\dot{\psi}$ . We fixed the potential assuming a circular velocity of  $250 \text{ km s}^{-1}$  at  $r = 1 \text{ kpc}$ . Following Mathews (1990) we took an equilibrium radius for the gaseous nebula  $a_{eq} = 0.37 \text{ pc}$ . It results that  $\ddot{\psi} < 0$  and  $\ddot{r} > 0$ : the clouds spiralize towards the galaxy center as expected. Moreover the drag effects are greater on faster starting clouds and therefore negligible for the slowly moving clouds in the very inner region of NGC 4036.

If the nebulae are homogeneously distributed in the gaseous spheroid only the tangential component  $r\dot{\psi}$  of their velocity contribute to the observed velocity. No contribution derives from the radial component  $\dot{r}$  of their velocities. In fact for each nebula moving towards the galaxy center, which is also approaching to us, we expect to find along the line-of-sight a receding nebula, which is falling towards the center from the same galactocentric distance with an opposite line-of-sight component of its  $\dot{r}$ . However the radial components of the cloudlets velocities (typically of  $30\text{-}40 \text{ km s}^{-1}$ ) are crucial to explain the velocity dispersion profile and to understand how the difference between the observed velocity dispersions and the model B predictions arises. If the clouds are decelerated by the drag force their orbits become more radially extended and the velocity ellipsoids acquire a radial anisotropy.

So we expect that (in the region of the gaseous spheroid) including drag effects in our gas modeling should give a velocity dispersion profile steeper than the one predicted by our isotropic model B, and in better agreement with observations.

## 5. Discussion and conclusions

The modeling of the stellar and gas kinematics in NGC 4036 shows that the observed velocities of the ionized gas, moving in the gravitational potential determined from the stellar kinematics, can not be explained without taking the gas velocity dispersion into account. In the inner regions of NGC 4036 the gas is not moving at circular velocity.

A better match with the observed gas kinematics is found by assuming the ionized gas as made of collisionless clouds in a spheroidal and disk component for which the Jeans Equations can be solved in the gravitational potential of the stars (i.e., model A). A much better agreement is achieved by assuming that the ionized gas emission comes from material which has recently been shed from the bulge stars (i.e., model B). If this gas is heated to the virial temperature of the galaxy (ceasing to produce emission lines) within a time much shorter than the orbital time, it shares the same ‘true’ kinematics of its parent stars. If this is the case we would observe a different kinematics for ionized gas and stars due only to their different spatial distribution. An HST H $\alpha$ +[N II] image of the nucleus of NGC 4036 confirms that except for a complex emission structure inside 3'' the smoothness of the distribution of the emission as we expect for the gas spheroidal component.

This kinematical modeling leaves open the questions about the physical state (e.g. the lifetime of the emitting clouds) and the origin of the dynamically hot gas. We tested the hypothesis that the ionized gas is located in short-living clouds shed by evolved stars (e.g. Mathews 1990) finding a satisfying agreement with our observational data. These clouds may be ionized by the parent stars, by shocks, or by the UV-flux from hot stars (Bertola *et al.* 1995a). The comparison with the more recent and detailed data on gas by Fisher (1997) opens wide the possibility for further modeling improvement if the drag effects on gaseous clouplets (due to the diffuse interstellar medium) will be taken into account. These arguments indicate that the dynamically hot gas in NGC 4036 has an internal origin. This does not exclude the possibility for the gaseous disk to be of external origin as discussed for S0's by Bertola *et al.* (1992). Spectra at higher spatial resolution are needed to understand the structure of the gas inside 3''.

## REFERENCES

- BERTOLA, F., BETTONI, D., RUSCONI, L. & SEDMAK, G. 1984, *AJ* **89**, 356  
 BERTOLA, F., BUSON, L.M. & ZEILINGER, W.W. 1992, *ApJ* **401**, L79  
 BERTOLA, F., BRESSAN, A., BURSTEIN, D. ET AL. 1995, *ApJ* **438**, 680  
 BERTOLA, F., CINZANO, P., CORSINI, E.M., RIX, H.-W. & ZEILINGER, W.W. 1995, *ApJ* **448**, L13  
 BINNEY, J.J., DAVIES, R.L. & ILLINGWORTH, G.D. 1990, *ApJ* **361**, 78  
 CINZANO, P. & VAN DER MAREL, R.P. 1994, *MNRAS* **270**, 325  
 DE VAUCOULEURS, G. ET AL. 1991, Third Reference Catalogue of Bright Galaxies. Springer-Verlag, New York (RC3)  
 FILLMORE, J.A., BOROSON, T.A. & DRESSLER, A. 1986, *ApJ* **302**, 208  
 FISHER, D. 1997, *AJ* **113**, 950  
 KORMENDY, J. & WESTPFahl, D.J. 1989, *ApJ* **338**, 772  
 MATHEWS, W.G. 1990, *ApJ* **354**, 468  
 SANDAGE, A. & TAMMANN, G.A. 1981, A Revised Shapley-Ames Catalog of Bright Galaxies. Carnegie Institution, Washington (RSA)  
 VAN DER MAREL, R.P. 1991, *MNRAS* **253**, 710  
 VAN DER MAREL, R.P., BINNEY, J.J. & DAVIES, R.L. 1990, *MNRAS* **245**, 582